Double Anisotropic Coherent Backscattering of Light

PHILIPP KRAUTER[1,*], CHRISTIAN ZOLLER[1], AND ALWIN KIENLE[1]

[1] *Institut für Lasertechnologien in der Medizin und Meßtechnik, Helmholtzstraße 12, D-89081 Ulm, Germany*
[*] *Corresponding author: philipp.krauter@gmx.de*

Compiled March 7, 2018

A double anisotropic coherent backscattering cone was found. In contrast to the (single) anisotropic coherent backscattering, which was observed in liquid crystals, here, the long axis of the elongated structures changes its orientation with angular distance. We compared our results with the 2-dimensional Fourier transform of spatially resolved reflectance measurements and found a good agreement which is predicted by the reciprocity thesis. Furthermore, a Monte Carlo model was applied to reproduce successfully the results of the experiment, whereas the double anisotropy is not predicted by diffusion models.

OCIS codes: (290.7050) Turbid media; (270.1670) Coherent optical effects; (290.4210) Multiple scattering; (160.1190) Anisotropic optical materials.

http://dx.doi.org/10.1364/ao.XX.XXXXXX

Measuring the propagation of light in scattering media is a usable tool for various fields of research. In spectroscopy, process control in scattering media and in medical diagnostics, an understanding and description of the light propagation is crucial. It can be described using a diffusion model as a simple approach or by the more sophisticated radiative transfer theory. Both models are based on statistical parameters and neglect wave phenomena such as interference. However, the coherent backscattering (CBS, also called "weak localization" [1–4]) survives multiple scattering and averaging over a broad spectrum [5]. Interestingly, the shape of the CBS signal which is obtained in the angular domain is closely related to the Fourier transform (FT) of the spatially resolved reflectance (SRR) that can be described by a purely incoherent theory [6]. That is, however, only an approximation, as will be discussed later. A theoretical explanation of the CBS effect was given many years ago e.g. by Akkermans et al. [6]. Anisotropic media was first examined with CBS only a few years later as a quasi two dimensional system [7]. About two decades after the isotropic CBS, an anisotropic CBS was found [8]. Most studies on anisotropic light propagation in CBS are dealing with nematic crystals [8–10]. Despite the fascination that the control of the matrix by an external field offers, they only reveal a small anisotropy in the detected CBS cone that can be described by the anisotropic diffusion equation [11, 12]. Other studies used strongly scattering etched gallium phosphide samples [13] and fitted the results well with the anisotropic diffusion equation. In the spatial domain, experiments on strongly anisotropic materials have revealed a more complex 2D reflectance [14–16]. In this study, we present for the first time a double anisotropic CBS measurement and a general model for its theoretical description.

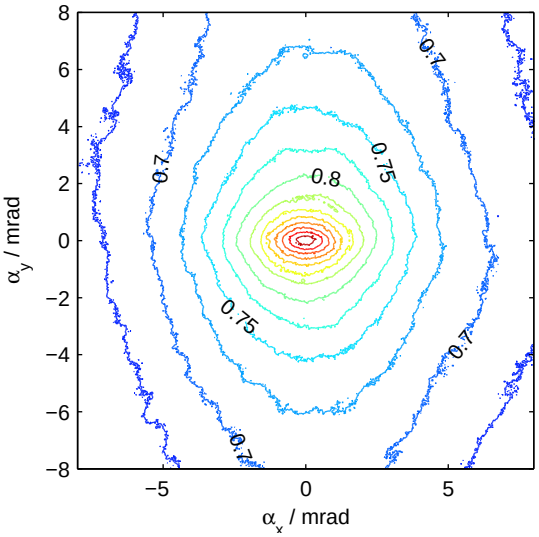

Fig. 1. Measurement of coherent backscattering cone of European hornbeam. Mean of vertical and horizontal polarization.

In Fig. 1 and 2, measurements of the double anisotropic coherent backscattering signal of European hornbeam (Carpinus betulus) and Norway maple (Acer platanoides) are shown. A double anisotropic CBS is observed showing iso-intensity lines elongated parallel to the underlying microstructure (the wood's tracheae in y-direction) at large angles and perpendicularly to the microstructure at small angles. Maxima are normalized to 1. In the following, we describe the setup to measure the CBS cone in detail. We then write on the setup to measure the SRR and display the results in this domain we obtained for the same sample of European hornbeam. Afterwards, the MC model to quantitatively reproduce the experimental results is presented and the results of the measurements and the simulation of European hornbeam are compared.

A scheme of the setup for measuring the CBS is shown in Fig. 3. A supercontinuum light source (Fianium SC450-6) is used to generate white light of which $\lambda = 550\,\text{nm}$ is extracted by means of an acousto optical tunable filter (Fianium AOTF). A single mode fiber transports the partly polarized light to a linear polarizer to ensure the polarization state. A lens system focuses the beam onto a 10 µm pinhole. This pinhole is imaged to infinity by

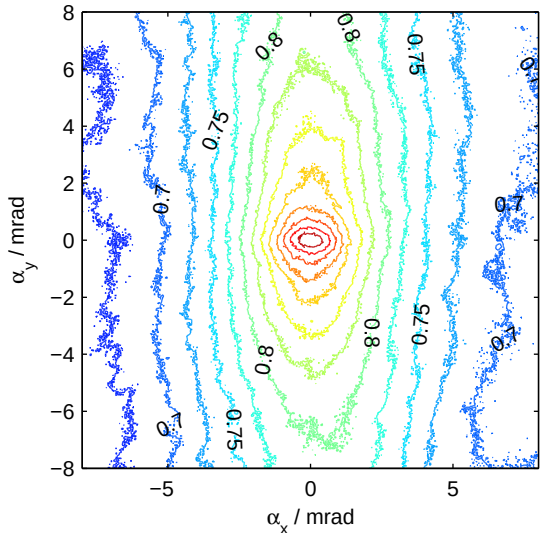

Fig. 2. Measurement of the coherent backscattering cone of Norway maple.

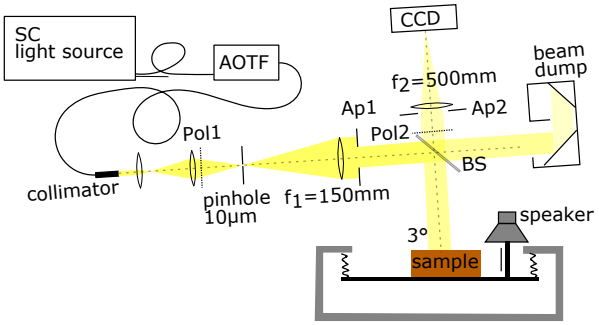

Fig. 3. Schematic of experimental setup for measuring the coherent backscattering cone. SC: supercontinuum, AOTF: acousto-optical tunable filter, Pol: polarizer, Ap: aperture, BS: beam splitter.

a $f = 150\,\mathrm{mm}$ achromatic lens. Using a 50:50 beam splitter, half of the collimated beam is sent onto the sample. The other part vanishes in the beam dump. The sample is illuminated by the collimated beam in an angle of 3° to the normal in order to avoid specular reflections on well-polished or liquid samples. A part of the reflected light passes the beam splitter and a polarization analyzer before it is imaged into angles by an achromatic lens with a focal length of $f = 500\,\mathrm{mm}$. In the focal plane of this lens, a CCD camera (QSI 640s) detects the angularly resolved light quantitatively. Since we want to measure the sample's anisotropy, we could not rotate the sample to efficiently reduce the speckle pattern as reported elsewhere [17–19]. Thus, the sample holder is vibrated by means of a speaker. To determine the angular resolution of the system, we printed a grating of crossed lines in distances of 400 µm on an overhead slide fixed to a mirror. With the CCD, several maxima can be observed in the angular space that are used for angular calibration. The analysis of a peak's shape leads to an angular FWHM of $\approx 90\,\mu\mathrm{rad}$ which is taken as an upper limit for the angular resolution. To account for the angular sensitivity of the detection system, we measured an epoxy resin optical phantom [20] having a reduced optical scattering coefficient $\mu_s' = 6\,\mathrm{mm}^{-1}$, for which the CBS cone is smaller than 1.5 mrad. Outside that region, CBS cones are corrected by the mostly incoherent part of said measurement.

In Fig. 1, we report the measurement of the double anisotropy in the CBS cone of European hornbeam (relative intensity), averaged over two orthogonal linear polarizations. This light-colored and dense hardwood has a large number of wood fibers and fine vessel elements such that the scattering is expected to be several times higher than that of softwood and thus gives rise to a angularly larger CBS cone that can be resolved more easily [21]. Both samples represent tangential sections from the trunk. The wood was dried for several years before the samples were cut out by a diamond saw blade. No sanding was applied. Although using unpolarized light would render the comparison of the CBS with the SRR easier, in order to increase the coherent enhancement factor E, we measured the polarization conserving channel of the linear polarization which breaks the radial asymmetry. However, we found this break negligible compared to the double anisotropy of the wood fibers, that dominates in both orientation of the polarization parallel and perpendicular to the wood fibers. The detected signal γ is the overlay of the incoherent background $\gamma_{\mathrm{incoh.}}$ and the CBS cone $\gamma_{\mathrm{CBS}}(\alpha)$ and can be written as $\gamma = \gamma_{\mathrm{incoh.}} + E\gamma_{\mathrm{CBS}}(\alpha)$ with the enhancement factor E. The incoherent background $\gamma_{\mathrm{incoh.}}$ is assumed to be constant over the relatively small angular field of view of $\approx 1°\mathrm{x}1°$. In most cases, this is a good approximation. We also found a double anisotropy for other wood types. In the CBS measurement of light-colored Norway maple (Fig. 2), the double anisotropy is clearly visible, moreover, the high-frequency iso-intensity lines form structures that are more elongated compared to the measurement of hornbeam. The angular field of view is too small to record the complete CBS cone. Thus, in the following comparisons, we consider the measurements on hornbeam. A noticeable double anisotropy was also found in the CBS measurement of beech. For mahogany, oak and Sibirian larch, it could be observed for some of the measurement locations, not for all, probably due to the nonregular growth of these wood types. For cherry wood, we found a strong anisotropy for larger angles, however, we were not able to resolve the double anisotropic structure probably due to its reddish color and the low reflectance at $\lambda = 550\,\mathrm{nm}$ of $\approx 25\,\%$.

For the measurement of the SRR, light of a xenon lamp is spectrally filtered by means of a grating with automated adjustment and $\lambda = 550\,\mathrm{nm}$ is coupled into an optical fiber. The end of this fiber is put directly on a 25 µm pinhole. The pinhole is imaged via an $f = 100\,\mathrm{mm}$ prime lens on the sample's surface at an angle of 23° to the normal. Using an $f = 80\,\mathrm{mm}$ achromatic lens, the surface of the sample is imaged on the sensor of a 4 megapixel sCMOS camera. We separately measure the radially symmetric system's function, i.e. the convolution of the incident beam with the transfer functions of the optics, by using a sand-blasted aluminum surface as sample. Please note that no polarizing element is used in the measurement of the SRR.

In Fig. 4a and b we present the experimental SRR image of the sample of European hornbeam and the deconvolved FT, respectively. For the deconvolution, the FT of Fig. 4a is divided pixelwise by the FT of the radially symmetric system's function. In the ideal case, the system's function would be $\delta(\vec{r})$ such that its FT would not depend on the frequency. In a real setup, it decreases with increasing frequency. If it falls below 15 % of its maximum, the values are not regarded anymore in Fig. 4b. In the spatial domain, the double anisotropy was reported for

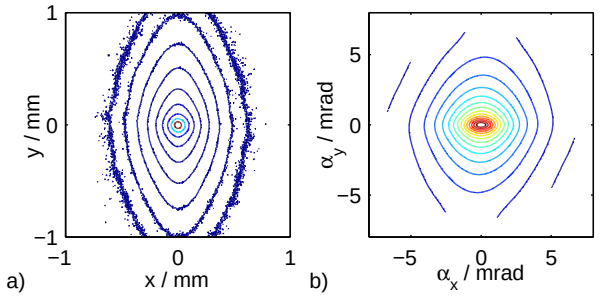

Fig. 4. Measurement of the 2D spatially resolved reflectance of European hornbeam (a) and its 2D-Fourier transform deconvolved by the systems function (b). The scaling of the iso-intensity lines is identical to Fig. 5.

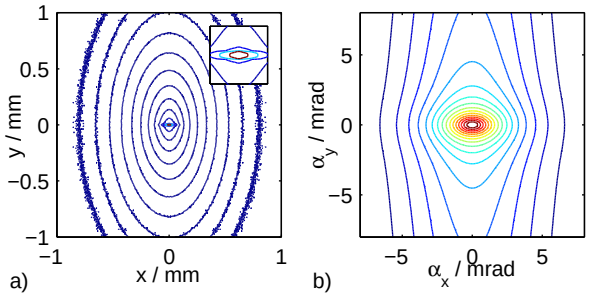

Fig. 5. Monte Carlo simulation of the dry wood model showing the double anisotropy in the spatial domain (a) and in the frequency domain (b) obtained by Fourier transformation. The spatial domain iso-intensity lines are logarithmically scaled with a factor of 3.16. The inset magnifies the central region, its total width is 100 µm. In (b), lines are linearly scaled ranging from 20 % to 95 % of the maximum in steps of 5 %.

anisotropic structures such as most wood types and many biological tissues such as ligaments [16], skin [22, 23], dentin [24], enamel, muscle, bone [23], tendon and nerve tissue.

The MC model being a solution to the radiative transfer equation is able to predict the double anisotropy when e.g. aligned cylinders are incorporated parallel to the surface. It is based on a model formerly introduced by Kienle et al. [15] for dry wood. In our model, scattering is due to parallel aligned fibers and, in addition, scatterers with properties that are independent of the direction of the incident light. The first are assumed to be cylindrical walls of xylem ($n = 1.55 + 0\,\mathrm{i}$) with an inner diameter of 3 µm filled with air ($n = 1.0$). The latter are assumed to be Henyey-Greenstein type scatterers having an anisotropy value of $g = 0.5$ which account for the non-aligned microstructure [25]. An effective refractive index of $n = 1.50$ is assumed with homogeneously distributed absorption. The illumination is pointlike and perpendicular to the surface. The remitted light is detected spatially resolved with an acceptance angle of 15°. To reproduce the CBS experiment, 1° would be more appropriate, however, the signal to noise ratio would suffer. To account for the insensitivity of the CBS to single scattering events, the simulation accepts only rays that are at least scattered twice. The contribution of the Henyey-Greenstein scatterers to the reduced scattering coefficient $\mu'_{\mathrm{s,iso}}$, the absorption coefficient μ_{a} and the number of fibers per mm^2 c_{cyl} were adjusted such that the FT of the simulation's SRR fits the coherent part of the CBS signal for angles up to 4 mrad yielding the optical properties $\mu'_{\mathrm{s,iso}} = 18.35\,\mathrm{mm}^{-1}$, $\mu_{\mathrm{a}} = 0.237\,\mathrm{mm}^{-1}$ and $c_{\mathrm{cyl}} = 34\,630\,\mathrm{mm}^{-2}$. Using these parameters, the simulated SRR and its FT are shown in Fig. 5.

The wood fibers in the MC model as well as in the experimental data are aligned parallel to the y-axis. In Fig. 5a we present the SRR of the MC model. In Fig. 5b we show the FT of Fig. 5a. The frequency axes f were replaced by the corresponding angles α using the relation $\alpha = \lambda f$ valid for small angles and $\lambda = 550\,\mathrm{nm}$ as applied in the experiments. The orientations of the double anisotropy in the spatial and the Fourier domain are identical. However, in the used model, the shape differs massively. In the Fourier domain, the elongation of the outermost iso-intensity curves is much larger compared to the spatial domain. Those "high-frequency" lines correspond to the high intensity lines in the spatial domain, only visible in the inset of Fig. 5a.

The 2D-patterns of the angular domains (CBS, SRR, MC) agree quite well qualitatively, compare Figs. 1 and 2 with Figs. 4b and 5b. Despite the complexity of the wood's microstructure, the simple MC model consisting only of aligned and non-aligned scatterers helps understanding the origin of the double anisotropy. A quantitative comparison in the angular domain is shown in Fig. 6. To achieve similar scaled values, we manually fit the enhancement factor E and shift the normalized (maximum=1) FTs of the SRR signal and MC simulation γ_{FT} to $(1 + E\gamma_{\mathrm{FT}})/(1 + E)$. The best agreement can be found for $E = 0.61$. This value separates the CBS signal in an incoherent and a coherent part that was applied for the optical property determination using the MC model. For angles up to 4 mrad, a good agreement of the FT of the spatial and CBS domain is found. Please note that the intersection point for both axes is not changed by the scaling. In the inlet, an angular range of 1 mrad is displayed around this special position. The intersection point seems to differ less than the CBS resolution of 0.1 mrad. For larger angles, the deviation get more pronounced which is probably due to the critical deconvolution of the SRR and the flatfield correction of the CBS image which produces an asymmetry between the left and the right side of the graph (compare Fig. 1).

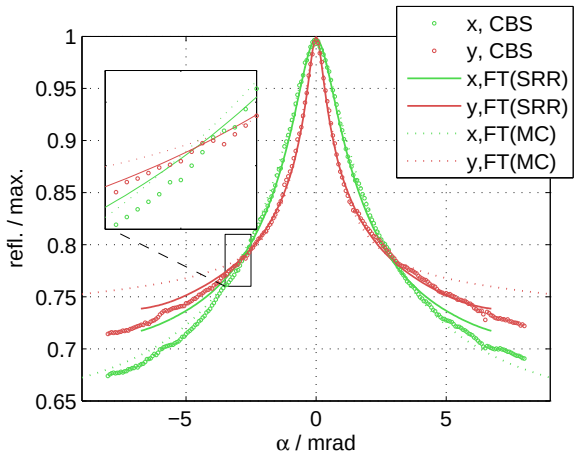

Fig. 6. Comparison of coherent backscattering CBS, Fourier transform of spatially resolved reflectance FT(SRR) of the same piece of European hornbeam parallel (x) and perpendicular (y) to the wood fibers as well as the best fit of the Monte Carlo simulation MC.

The result for the MC simulation and the CBS measurement

agree well for angles up to 3 mrad. This area is smaller than the 4 mrad that were used for the optical properties determination in the MC model. For larger angles, the reflectance perpendicular (x-direction) to the fiber's orientation still shows a good agreement, however, parallel to the fibers (y-direction), the MC simulation reveals reflectance values higher than in the experiment. An explanation for this deviation can be found in Fig. 5a with the inset magnifying the center of the image. There, an extremly sharp increase of the reflectance perpendicular to the fibers' orientation can be found. In the MC model, a bin width of 5 µm was used, however, the central bin was still an order of magnitude brighter than its neighbor in y-direction. Although only a handful of bins are that bright, for larger frequencies, they become dominant and increase the Fourier transformed signal in the direction parallel to the fibers. The origin for these very bright bins is mainly low order scattering solely by cylinders. Due to the perpendicular incidence in the MC model, light is scattered only in the xz-plane until a Henyey-Greenstein scattering event takes place. Combined with the pointlike illumination, it renders a discontinuity no matter how fine the bins are. In the CBS and SRR experiments, the illumination is oblique with angles of 3° and $\approx$ 20°, respectively. If the oblique incidence is in the yz-plane, light scattered solely by cylinders keeps its y-component of the propagation vector, such that its reflectance is not localized in 1D and, thus, is not detected by the numerical apertures of the detetors. If the sample (and the coordinate system) is rotated, the incidence is in the xz-plane such that light can be backscattered and thus contribute to the signal. Please note that in both experiments, the wood sample was rotated by 90° and the average reflectance image is presented.

In conclusion, we presented the first measurements of the double anisotropy (orientation of elongation of iso-intensity lines changes with frequency) in the coherent backscattering cone. In literature, a small (single) anisotropy in the CBS was reported that could be described well by the anisotropic diffusion equation. With increasing anisotropy of the scattering tensor, the elliptical iso-intensity lines of the diffusive solution become more and more elongated. If the structures are strongly aligned, we showed that the double anisotropy appears which cannot be described by diffusion anymore. This feature is not predicted by the diffusion equation since it requires a more detailed physical model for considering the medium's microstructure. In addition, using a reduced scattering tensor, it is not possible to describe the angular function of μ_s' for the cylinders in our Monte Carlo (MC) model. We found the latter to be maximal for an angle of 50° (contribution of cylinders: $\mu_s' = 58.2\,\mathrm{mm}^{-1}$) between the cylinder's axis and incident light which then decreases to $\mu_s' = 41\,\mathrm{mm}^{-1}$ for perpendicular incidence. The Monte Carlo model's generality allows for its application on other anisotropic media. On the other hand, more material-specific models for example considering birefringence might further increase the simulation accuracy and would be well-suited to describe the influence of the wood's anisotropic elements on the light propagation seperately.

We found a good agreement of the CBS double anisotropic cone with the Fourier transform of the spatially resolved reflectance measurement of the same sample of European hornbeam. The agreement is astonishing although several effects to disturb the simple Fourier connection are obvious. First of all, both experiments use different geometries for incident and detected light. Secondly, the existence of the CBS cone changes the light propagation since it increases the total reflectance (weak localization) and only occurs when the sample is illuminated in a wide area. Thirdly, in the CBS measurement, we only detected the polarization conserving channel of a linearly polarized incidence and finally, in contrast to the CBS, in the SRR, single scattered light contributes to the signal. The latter is, however, not relevant, since single scattered light contributes mainly to a constant over the angular field of view. Thus, it cannot be separated from the incoherent reflectance background and only changes the experimental enhancement factor of $E = 0.61$. Adjusted optical parameters render a similar reflectance in Monte Carlo simulations compared to both experiments.

Especially for strongly scattering media, the measurement of the CBS seems to be a well-suited method to determine the reflectance profile for anisotropic media and obtain optical properties using an appropriate model. The presented method can also be applied to detect structural changes, in particular in many biological tissues such as skin, muscle, bone, tendon, ligaments and nerve tissue, e.g. for early cancer detection. Moreover, since CBS is a classical wave phenomenon, the double anisotropy might be found in other types of waves as well.

The authors acknowledge the support of the Deutsche Forschungsgemeinschaft, P. Krauter acknowledges the support by Evangelisches Studienwerk Villigst e.V.

REFERENCES

1. Y. Kuga and A. Ishimaru, JOSA A **1**, 831 (1984).
2. M. P. Van Albada and A. Lagendijk, Physical Review Letters **55**, 2692 (1985).
3. P.-E. Wolf and G. Maret, Physical Review Letters **55**, 2696 (1985).
4. M. Kaveh, M. Rosenbluh, I. Edrei, and I. Freund, Physical Review Letters **57**, 2049 (1986).
5. T. Gehrels, The Astrophysical Journal **123**, 331 (1956).
6. E. Akkermans, P. Wolf, R. Maynard, and G. Maret, Journal de Physique **49**, 77 (1988).
7. I. Freund, M. Rosenbluh, R. Berkovits, and M. Kaveh, Physical Review Letters **61**, 1214 (1988).
8. R. Sapienza, S. Mujumdar, C. Cheung, A. Yodh, and D. Wiersma, Physical Review Letters **92**, 033903 (2004).
9. H. Vithana, L. Asfaw, and D. Johnson, Physical review letters **70**, 3561 (1993).
10. E. Aksenova, D. Kokorin, and V. Romanov, Physical Review E **89**, 052506 (2014).
11. A. Kienle, Physical Review Letters **98**, 218104 (2007).
12. E. Alerstam, Physical Review E **89**, 063202 (2014).
13. B. Bret and A. Lagendijk, Physical Review E **70**, 036601 (2004).
14. A. Kienle, F. Forster, and R. Hibst, Optics letters **29**, 2617 (2004).
15. A. Kienle, C. D'Andrea, F. Foschum, P. Taroni, and A. Pifferi, Optics Express **16**, 9895 (2008).
16. E. Simon, P. Krauter, and A. Kienle, J. Biomed. Opt. **19**, 075006 (2014).
17. D. S. Wiersma, M. P. van Albada, B. A. van Tiggelen, and A. Lagendijk, Physical Review Letters **74**, 4193 (1995).
18. D. Wiersma, M. P. van Albada, and A. Lagendijk, Review of Scientific Instruments **66**, 5473 (1995).
19. P. Gross, M. Störzer, S. Fiebig, M. Clausen, G. Maret, and C. M. Aegerter, Review of Scientific Instruments **78**, 033105 (2007).
20. P. Krauter, S. Nothelfer, N. Bodenschatz, E. Simon, S. Stocker, F. Foschum, and A. Kienle, Journal of Biomedical Optics **20**, 105008 (2015).
21. W. Schoch, I. Heller, F. Schweingruber, and F. Kienast, "Wood anatomy of central european species," Online version www.woodanatomy.ch (2004).
22. S. Nickell, M. Hermann, M. Essenpreis, T. J. Farrell, U. Krämer, and M. S. Patterson, Phys. Med. Biol. **45**, 2873 (2000).
23. A. Sviridov, V. Chernomordik, M. Hassan, A. Russo, A. Eidsath, P. Smith, and A. H. Gandjbakhche, Journal of Biomedical Optics **10**, 014012 (2005).
24. A. Kienle and R. Hibst, Physical Review Letters **97**, 018104 (2006).
25. L. Henyey and J. Greenstein, The Astrophysical Journal **93**, 70 (1941).

REFERENCES

1. Yasuo Kuga and Akira Ishimaru. Retroreflectance from a dense distribution of spherical particles. *JOSA A*, 1(8):831–835, 1984.
2. Meint P Van Albada and Ad Lagendijk. Observation of weak localization of light in a random medium. *Physical Review Letters*, 55(24):2692, 1985.
3. Pierre-Etienne Wolf and Georg Maret. Weak localization and coherent backscattering of photons in disordered media. *Physical Review Letters*, 55(24):2696, 1985.
4. M Kaveh, M Rosenbluh, I Edrei, and I Freund. Weak localization and light scattering from disordered solids. *Physical Review Letters*, 57(16):2049, 1986.
5. Thomas Gehrels. Photometric studies of asteroids. v. the light-curve and phase function of 20 massalia. *The Astrophysical Journal*, 123:331, 1956.
6. E Akkermans, PE Wolf, R Maynard, and G Maret. Theoretical study of the coherent backscattering of light by disordered media. *Journal de Physique*, 49(1):77–98, 1988.
7. Isaac Freund, Michael Rosenbluh, Richard Berkovits, and Moshe Kaveh. Coherent backscattering of light in a quasi-two-dimensional system. *Physical Review Letters*, 61(10):1214, 1988.
8. Riccardo Sapienza, Sushil Mujumdar, Cecil Cheung, AG Yodh, and Diederik Wiersma. Anisotropic weak localization of light. *Physical Review Letters*, 92(3):033903, 2004.
9. HKM Vithana, L Asfaw, and DL Johnson. Coherent backscattering of light in a nematic liquid crystal. *Physical review letters*, 70(23):3561, 1993.
10. EV Aksenova, DI Kokorin, and VP Romanov. Simulation of radiation transfer and coherent backscattering in nematic liquid crystals. *Physical Review E*, 89(5):052506, 2014.
11. Alwin Kienle. Anisotropic light diffusion: an oxymoron? *Physical Review Letters*, 98(21):218104, 2007.
12. Erik Alerstam. Anisotropic diffusive transport: Connecting microscopic scattering and macroscopic transport properties. *Physical Review E*, 89(6):063202, 2014.
13. BPJ Bret and Aart Lagendijk. Anisotropic enhanced backscattering induced by anisotropic diffusion. *Physical Review E*, 70(3):036601, 2004.
14. A Kienle, FK Forster, and R Hibst. Anisotropy of light propagation in biological tissue. *Optics letters*, 29(22):2617–2619, 2004.
15. Alwin Kienle, Cosimo D'Andrea, Florian Foschum, Paola Taroni, and Antonio Pifferi. Light propagation in dry and wet softwood. *Optics Express*, 16(13):9895–9906, 2008.
16. Emanuel Simon, Philipp Krauter, and Alwin Kienle. Time-resolved measurements of the optical properties of fibrous media using the anisotropic diffusion equation. *J. Biomed. Opt.*, 19(7):075006, 2014.
17. Diederik S Wiersma, Meint P van Albada, Bart A van Tiggelen, and Ad Lagendijk. Experimental evidence for recurrent multiple scattering events of light in disordered media. *Physical Review Letters*, 74(21):4193, 1995.
18. DS Wiersma, Meint P van Albada, and Ad Lagendijk. An accurate technique to record the angular distribution of backscattered light. *Review of Scientific Instruments*, 66(12):5473–5476, 1995.
19. Peter Gross, Martin Störzer, Susanne Fiebig, Martin Clausen, Georg Maret, and Christof M Aegerter. A precise method to determine the angular distribution of backscattered light to high angles. *Review of Scientific Instruments*, 78(3):033105, 2007.
20. Philipp Krauter, Steffen Nothelfer, Nico Bodenschatz, Emanuel Simon, Sabrina Stocker, Florian Foschum, and Alwin Kienle. Optical phantoms with adjustable subdiffusive scattering parameters. *Journal of Biomedical Optics*, 20(10):105008, 2015.
21. W. Schoch, I. Heller, F.H. Schweingruber, and F. Kienast. Wood anatomy of central european species. Online version www.woodanatomy.ch, 2004.
22. Stephan Nickell, Marcus Hermann, Matthias Essenpreis, Thomas J Farrell, Uwe Krämer, and Michael S Patterson. Anisotropy of light propagation in human skin. *Phys. Med. Biol.*, 45(10):2873, 2000.
23. Alexander Sviridov, Victor Chernomordik, Moinuddin Hassan, Angelo Russo, Alec Eidsath, Paul Smith, and Amir H Gandjbakhche. Intensity profiles of linearly polarized light backscattered from skin and tissue-like phantoms. *Journal of Biomedical Optics*, 10(1):014012–0140129, 2005.
24. Alwin Kienle and Raimund Hibst. Light guiding in biological tissue due to scattering. *Physical Review Letters*, 97(1):018104, 2006.
25. L.G. Henyey and J.L. Greenstein. Diffuse radiation in the galaxy. *The Astrophysical Journal*, 93:70–83, 1941.